[3]R. Blankenbecler and L. F. Cook, Jr., Phys. Rev. 119, 1745 (1960).
[4]R. D. Amado, Phys. Rev. 132, 485 (1963).
[5]S. Weinberg, Phys. Rev. 133, B1318 (1964); 134, B882 (1964).
[6]H. Pagels, Phys. Rev. 144, 1250 (1966).
[7]This work uses natural units and the metric has a signature of −2. The Dirac equation reads $(\not{k}+M)u(k)=0$ and $\sigma_{\mu\nu}=i(\gamma_\mu\gamma_\nu-\gamma_\nu\gamma_\mu)/2$.
[8]S. Weinberg, Phys. Rev. 140, B516 (1965).
[9]A. M. Bincer, Phys. Rev. 118, 855 (1960).
[10]Our λ' is the λ of Ref. 1.
[11]See, for instance, S. S. Schweber, *An Introduction to Relativistic Quantum Field Theory* (Harper & Row, New York, 1962).
[12]R. Oehme, Phys. Rev. 100, 1503 (1955).
[13]M. Gourdin, M. Le Bellac, F. M. Renard, and J. Tran Thanh Van, Nuovo Cimento 37, 524 (1965).
[14]J. Mathews and B. Deo, Phys. Rev. 143, 1340 (1966).
[15]Ian Duck, Nucl. Phys. B1, 96 (1967).
[16]S. Drell and H. Pagels, Phys. Rev. 140, B397 (1965); R. G. Parson, *ibid.* 168, 1562 (1968).

PHYSICAL REVIEW D VOLUME 4, NUMBER 3 1 AUGUST 1971

Evidence on Duality and Exchange Degeneracy from Finite-Energy Sum Rules: $K^-n\to\pi^-\Lambda$ and $\pi^+n\to K^+\Lambda$†

R. D. Field, Jr. and J. D. Jackson
Department of Physics and Lawrence Radiation Laboratory, University of California, Berkeley, California 94720
(Received 5 April 1971)

Using finite-energy sum rules for the reactions $K^-n\to\pi^-\Lambda$ and $\pi^+n\to K^+\Lambda$, we determine the effective "pole" parameters of the K^* and K^{**} Regge trajectories from a knowledge of the low-energy resonances and their couplings. The resonance parameters and the $D/(D+F)$ ratio for the $\frac{1}{2}^+$ baryon octet are varied somewhat to test the sensitivity of the high-energy predictions; $\frac{1}{2}^+$ octet couplings within the range of values found empirically in other reactions are preferred in our solution. We find that the s-channel resonances in $K^-n\to\pi^-\Lambda$ *do* add in such a way as to produce predominantly real amplitudes at high energies as predicted by duality diagrams. We find, however, that these predictions are not satisfied *exactly*. Although the phases of both A' and B are small and independent of t for $|t|<0.5$ (GeV/c)^2, the residues of the even- and odd-signature Regge poles are closely exchange-degenerate only for the B amplitudes, and not for the A' amplitudes, thereby allowing an appreciable polarization for $K^-n\to\pi^-\Lambda$ as is observed experimentally. The Regge-pole parameters determined from the sum rules give a good fit to the reaction $K^-n\to\pi^-\Lambda$ over a wide range of energies, whereas they are unable to fit $\pi^+n\to K^+\Lambda$ at intermediate energies. Comparison of the resonance contributions to $K^-n\to\pi^-\Lambda$ and $\pi^+n\to K^+\Lambda$ shows that "peripheral" resonances dominate the sum rules in the first reaction, while "nonperipheral" states are important in the second. By supposing that "peripheral" resonances are dual to the leading Regge singularities in the t channel, while "nonperipheral" resonances are dual to lower-lying singularities, we are led to a rationale of why the simple model of two effective Regge poles is adequate for $K^-n\to\pi^-\Lambda$ even at intermediate energies, but inadequate there for $\pi^+n\to K^+\Lambda$.

I. INTRODUCTION

The duality diagrams introduced by Harari[1] and Rosner[2] conveniently illustrate the ramifications of duality and the absence of quark-model "exotic" states. Processes with planar duality diagrams supposedly have high-energy amplitudes with imaginary parts and t-dependent phases, whereas reactions with nonplanar diagrams have purely real amplitudes at high energy. Rosner explicitly states that his derivation of the duality diagrams from $SU(3)$ couplings applies only to the nonflip amplitude (A') of (0^-, $\frac{1}{2}^+$) scattering, and requires purely f coupling of the vector mesons, and purely d coupling of the tensor mesons to the pseudoscalar mesons. Harari, on the other hand, conjectures that whenever a diagram is nonplanar all the corresponding helicity amplitudes should be purely real at high energies. Thus Harari predicts that whenever the duality diagram for a reaction is nonplanar the polarization should vanish at high energy. One such process is $K^-n\to\pi^-\Lambda$, whose three duality diagrams are shown in Fig. 1. Although the quantum numbers allow resonances in all three channels, the s-t diagram, relevant for near-forward scattering at high s, is nonplanar. Following Harari's conjecture that both the nonflip (A') and flip (B) amplitudes are real, we should expect no high-energy polarization. However, experiments at 3.0 and 4.5 GeV/c show a

large positive polarization for $0 \leq |t| \leq 1.5$ GeV/c.[3,4] In an effort to understand the origins of this apparent failure of duality diagrams and also the breaking of exchange degeneracy (EXD) for the reaction $K^-n \to \pi^-\Lambda$ and its line-reversed partner $\pi^+n \to K^+\Lambda$, already emphasized by Lai and Louie,[5] we present here an analysis of these inelastic processes in terms of finite-energy sum rules (FESR). Independent of these specific motives, we wish to elucidate the properties of hypercharge exchange in the t channel and to test the usefulness of FESR for inelastic reactions.

It is well known that the FESR are unable to distinguish among the various high-energy models. Hence one must know or assume what the model is at high energies. Then FESR can help determine parameters inside that framework. We adopt a conventional high-energy model consisting of two Regge "poles" in the t channel [see Fig. 1(d)], the $K^*(890)$ with negative signature and the $K^{**}(1420)$ with positive signature. The Regge "poles" are to be understood as effective poles into which the effects of branch cuts have been absorbed. We use the FESR to determine the residues of the two Regge poles and hence determine the high-energy behavior of the amplitudes A' and B. This leads to predictions of the differential cross section and polarization at high energy for the reaction $K^-n \to \pi^-\Lambda$ and the "line-reversed" reaction $\pi^+n \to K^+\Lambda$.

We start in Sec. II by giving a detailed discussion of use of FESR in the inelastic reaction $K^-n \to \pi^-\Lambda$. We define and discuss the use of signatured amplitudes and the necessity of daughter trajectories. We also present a discussion of the narrow-resonance approximation and questions concerning the resonances or poles below threshold and arbitrariness in their parameters. In Sec. III we exhibit and discuss the FESR results for the high-energy observables of $K^-n \to \pi^-\Lambda$, the status of EXD for the K^* and K^{**} exchanges and the associated reality of the amplitudes for $K^-n \to \pi^-\Lambda$, the EXD of the direct-channel $Y=0$, $I=1$ Σ^* resonances, the failure of the model at intermediate energies for $\pi^+n \to K^+\Lambda$, and possible reasons for it. A summary is given in Sec. IV.

The reader who is interested only in the results can begin with Sec. II C and Fig. 5 and proceed to Sec. IV.

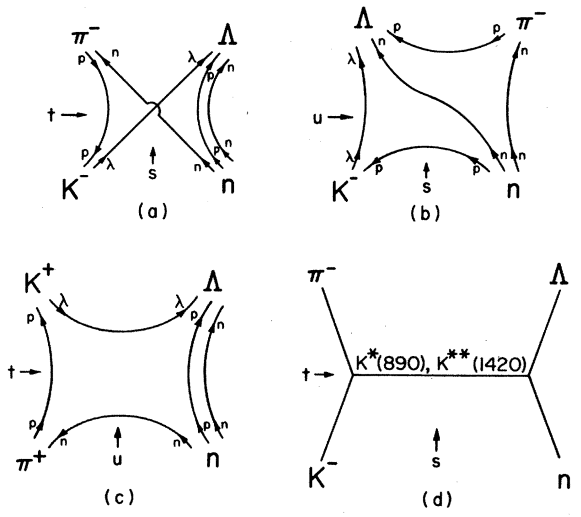

FIG. 1. Duality diagrams for $K^-n \to \pi^-\Lambda$: (a) Nonplanar s-t duality diagram; (b) and (c) planar s-u and u-t diagrams; (d) t-channel Regge exchanges.

II. APPLICATION OF FESR TO THE REACTION $K^-n \to \pi^-\Lambda$

A. Sum-Rule Formalism, Crossing versus Signature, High-Energy Observables

We employ integer-moment FESR of the standard form,[6]

$$\int_0^{\nu_1} d\nu\, \nu^n \mathrm{Im}F^{(\pm)}(\nu, t) = \int_0^{\nu_1} d\nu\, \nu^n \mathrm{Im}F^{(\pm)}_{\mathrm{asym}}(\nu, t), \tag{2.1}$$

where $F^{(\pm)}(\nu, t)$ is an appropriate reaction amplitude whose asymptotic form $F^{(\pm)}_{\mathrm{asym}}(\nu, t)$ is assumed to represent the amplitude for $|\nu| > \nu_1$. The integer n is even (odd) for amplitudes that are odd (even) under $\nu \to -\nu$.

The notation for the kinematics of the reaction, $K^-n \to \pi^-\Lambda$, and the crossed reaction, $\pi^+n \to K^+\Lambda$, is shown in Fig. 2. The amplitudes to be used in the FESR (2.1) are constructed from the invariant amplitudes A and B which enter the Feynman amplitude for the two reactions

$$\mathfrak{M}(p', q'; p, q) = \bar{U}_\Lambda(p')[-A(s,t,u) + \tfrac{1}{2}i\gamma\cdot(q+q')B(s,t,u)]U_n(p),$$

$$\mathfrak{M}(p', \bar{q}'; p, \bar{q}) = \bar{U}_\Lambda(p')[-\bar{A}(u,t,s) + \tfrac{1}{2}i\gamma\cdot(\bar{q}+\bar{q}')\bar{B}(u,t,s)]U_n(p).$$

Note that A and B correspond to the process $K^-n \to \pi^-\Lambda$, and $\bar{A}$ and $\bar{B}$ to $\pi^+n \to K^+\Lambda$, and also that $\bar{q}' = -q$, $\bar{q} = -q'$. The scale of $\mathfrak{M}$ is defined by the differential cross-section formula

$$\frac{d\sigma}{dt} = \frac{1}{64\pi s p^2}|\mathfrak{M}|^2,$$

where p is the center-of-mass momentum in the initial state, and a sum over final spins and an average over initial spins is understood. Using the crossing behavior of $\mathfrak{M}$,

$$\mathfrak{M}^*(p, -q'; p', -q) = \mathfrak{M}(p', q'; p, q),$$

we see that

$$\bar{A}^*(u, t, s) = A(s, t, u),$$

$$\bar{B}^*(u, t, s) = -B(s, t, u).$$

In terms of the variables $\nu = (s-u)/4m$ and t, and with the real analytic property of A and B, the crossing conditions are

$$\bar{A}(\nu + i\epsilon, t) = A(-\nu - i\epsilon, t), \tag{2.2a}$$

$$\bar{B}(\nu + i\epsilon, t) = -B(-\nu - i\epsilon, t). \tag{2.2b}$$

In the following we drop the $i\epsilon$ with the understanding that the physical regions for the two reactions are as indicated in Fig. 3.

Since we are dealing with Regge trajectories in the t channel, we introduce the t-channel helicity nonflip and flip amplitudes, respectively,

$$f^t_{++}(\nu, t) = \frac{(m+m')^2 A'(\nu, t)}{[t-(m+m')^2]^{1/2}},$$

$$f^t_{+-}(\nu, t) = \frac{[\phi(\nu, t)]^{1/2} B(\nu, t)}{[t-(m+m')^2]^{1/2}},$$

where $\phi(\nu, t) = 4tp_t^2 q_t^2 \sin^2\theta_t$ is the Kibble function. The amplitude A' is expressed in terms of A and B as follows:

$$A'(\nu, t) = \left[1 - \frac{t}{(m+m')^2}\right] A(\nu, t) + \frac{2m}{m+m'} \nu B(\nu, t) + \frac{1}{2} \frac{(m'-m)(\mu'^2 - \mu^2)}{(m+m')^2} B(\nu, t).$$

Similarly,

$$\bar{A}'(\nu, t) = \left[1 - \frac{t}{(m+m')^2}\right] \bar{A}(\nu, t) + \frac{2m}{m+m'} \nu \bar{B}(\nu, t) - \frac{1}{2} \frac{(m'-m)(\mu'^2 - \mu^2)}{(m+m')^2} \bar{B}(\nu, t).$$

For forward elastic scattering the above equation for A' reduces to $A' = A + \nu B$, which is the same amplitude as defined by Singh.[7] The crossing behavior of A' is easily seen to be

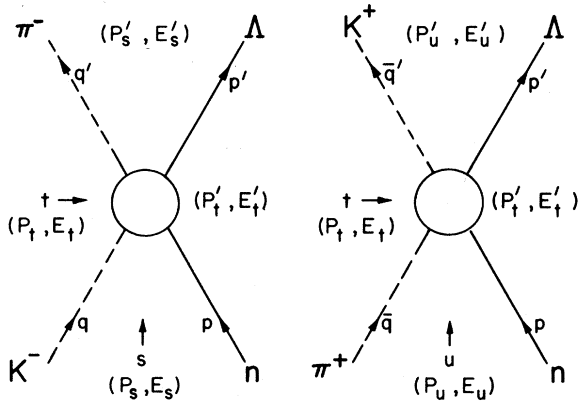

FIG. 2. Diagrams defining the kinematic variables for $K^- n \to \pi^- \Lambda$ and $\pi^+ n \to K^+ \Lambda$.

$$\bar{A}'(\nu, t) = A'(-\nu, t). \tag{2.3}$$

Amplitudes with even or odd behavior under $\nu \to -\nu$ may be formed in an obvious way:

$$A'^{(\pm)}(\nu, t) = \tfrac{1}{2}[A'(\nu, t) \pm A'(-\nu, t)] = \tfrac{1}{2}[A'(\nu, t) \pm \bar{A}'(\nu, t)], \tag{2.4a}$$

$$B^{(\pm)}(\nu, t) = \tfrac{1}{2}[B(\nu, t) \mp B(-\nu, t)] = \tfrac{1}{2}[B(\nu, t) \pm \bar{B}(\nu, t)], \tag{2.4b}$$

where the final expressions result from use of the crossing relations (2.2b) and (2.3).

In using finite-energy sum rules it is customary to assume that at high energies s the amplitudes are dominated by certain Regge trajectories (or at least effective Regge trajectories) of definite signature in the t channel. For elastic scattering, amplitudes with even or odd signature are also even or odd under $\nu \to -\nu$, but for inelastic processes this is not true in general. Amplitudes $\hat{A}'^{(\pm)}$ and $\hat{B}^{(\pm)}$ having definite signature in the t channel are formed as follows:

$$\hat{A}'^{(\pm)}(z_t, t) = \tfrac{1}{2}[A'(z_t, t) \pm A'(-z_t, t)] = \tfrac{1}{2}\sum_J (2J+1) A'^{(\pm)}(J, t)[P_J(z_t) \pm P_J(-z_t)],$$

$$\hat{B}^{(\pm)}(z_t, t) = \tfrac{1}{2}[B(z_t, t) \mp B(-z_t, t)] = -\tfrac{1}{2}\sum_J (2J+1) \frac{B^{(\pm)}(J, t)}{[J(J+1)]^{1/2}}[P_J'(z_t) \mp P_J'(-z_t)],$$

and are even or odd under $z_t \to -z_t$. The connection between z_t and the kinematic variables,

$$4p_t p_t' z_t = 4m\nu + (\mu'^2 - \mu^2)(m'^2 - m^2)/t,$$

shows that $z_t \to -z_t$ is the same as $\nu \to -\nu$ for processes in which $\mu' = \mu$ or $m' = m$ (or both), but not the same for the general inelastic process. This complication for arbitrary masses is just one aspect of the problems encountered in describing such processes in terms of Regge exchanges. It is well known that Freedman and Wang[8] assured power-law behavior at all t values and Mandelstam

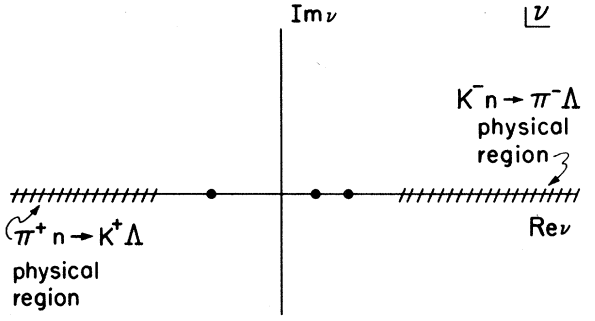

FIG. 3. Complex ν plane showing schematically the locations of poles, unitarity cuts, and the physical regions for $K^- n \to \pi^- \Lambda$ and the crossed reaction, $\pi^+ n \to K^+ \Lambda$.

analyticity near $t=0$ by the introduction of daughter trajectories. The basic Regge-pole contributions to the signatured amplitudes are

$$\hat{A}'^{(\pm)}(z_t, t) = \pi[\alpha^{\pm}(t) + \tfrac{1}{2}]\beta_a^{(\pm)}(t)P_{\alpha^{\pm}}(z_t)\xi^{\pm}(\alpha^{\pm}), \quad (2.5a)$$

$$\hat{B}^{(\pm)}(z_t, t) = -\pi[\alpha^{\pm}(t) + \tfrac{1}{2}]\beta_b^{(\pm)}(t)P_{\alpha^{\pm}}'(z_t)\xi^{\pm}(\alpha^{\pm}), \quad (2.5b)$$

where $\xi^{\pm}(\alpha)$ is the usual signature factor

$$\xi^{\pm}(\alpha) = [\pm 1 + e^{-i\pi\alpha(t)}]/[-\sin\pi\alpha(t)].$$

With the introduction of daughter trajectories, the Legendre function $P_\alpha(z_t)$ is replaced, to leading order in ν, as follows:

$$P_\alpha(z_t) \to \frac{\Gamma(\alpha+\frac{1}{2})}{(\pi)^{1/2}\Gamma(\alpha+1)}\left(\frac{2m\nu}{p_t p_t'}\right)^{\alpha},$$

$$P_\alpha'(z_t) \to \frac{\alpha\Gamma(\alpha+\frac{1}{2})}{(\pi)^{1/2}\Gamma(\alpha+1)}\left(\frac{p_t p_t'}{m\nu}\right)\left(\frac{2m\nu}{p_t p_t'}\right)^{\alpha}.$$

The high-energy behavior of $\hat{A}'^{(\pm)}$ and $\hat{B}^{(\pm)}$ then becomes

$$\hat{A}'^{(\pm)}_{\text{asym}}(z_t, t) = a^{\pm}(t)(\nu/\nu_0)^{\alpha^{\pm}}\xi^{\pm}(\alpha^{\pm}), \quad (2.6a)$$

$$\nu\hat{B}^{(\pm)}_{\text{asym}}(z_t, t) = b^{\pm}(t)(\nu/\nu_0)^{\alpha^{\pm}}\xi^{\pm}(\alpha^{\pm}), \quad (2.6b)$$

where

$$a^{\pm}(t) = \frac{(\pi)^{1/2}\Gamma(\alpha^{\pm}+\frac{3}{2})}{\Gamma(\alpha^{\pm}+1)}\left(\frac{2m\nu_0}{p_t p_t'}\right)^{\alpha^{\pm}}\beta_a^{(\pm)}(t), \quad (2.6c)$$

$$b^{\pm}(t) = \frac{-(\pi)^{1/2}\alpha^{\pm}(t)\Gamma(\alpha^{\pm}+\frac{3}{2})}{\Gamma(\alpha^{\pm}+1)}\left(\frac{p_t p_t'}{m}\right)\left(\frac{2m\nu_0}{p_t p_t'}\right)^{\alpha^{\pm}}\beta_b^{(\pm)}(t), \quad (2.6d)$$

and $\nu_0 \equiv s_0/2m$ is a scale factor. We see that the net result of incorporating daughters is to make the dominant contribution to the signatured amplitudes at high energy have definite crossing properties with respect to the energy variable ν, that is to say, that to leading order in ν,

$$A'^{(\pm)}_{\text{asym}}(\nu, t) = \hat{A}'^{(\pm)}_{\text{asym}}(\nu, t), \quad (2.7a)$$

$$B^{(\pm)}_{\text{asym}}(\nu, t) = \hat{B}^{(\pm)}_{\text{asym}}(\nu, t). \quad (2.7b)$$

When the above expressions for $\hat{A}'^{(\pm)}_{\text{asym}}$ and $\hat{B}^{(\pm)}_{\text{asym}}$ (2.6a) and (2.6b) and (2.7a) and (2.7b) are used, the sum rules for $A'^{(\pm)}$ and $\nu B^{(\pm)}$ are

$$S(A'^{(+)}, n) \equiv \frac{1}{\nu_1^{2n+2}}\int_0^{\nu_1}\nu^{2n+1}\text{Im}A'^{(+)}(\nu, t)d\nu = \frac{a^+(t)}{\alpha^+(t)+2n+2}\left(\frac{\nu_1}{\nu_0}\right)^{\alpha^+(t)}, \quad (2.8a)$$

$$S(A'^{(-)}, n) \equiv \frac{1}{\nu_1^{2n+1}}\int_0^{\nu_1}\nu^{2n}\text{Im}A'^{(-)}(\nu, t)d\nu = \frac{a^-(t)}{\alpha^-(t)+2n+1}\left(\frac{\nu_1}{\nu_0}\right)^{\alpha^-(t)}, \quad (2.8b)$$

$$S(B^{(+)}, n) \equiv \frac{1}{\nu_1^{2n}}\int_0^{\nu_1}\nu^{2n}\text{Im}B^{(+)}(\nu, t)d\nu = \frac{b^+(t)}{\alpha^+(t)+2n}\left(\frac{\nu_1}{\nu_0}\right)^{\alpha^+(t)}, \quad (2.8c)$$

$$S(B^{(-)}, n) \equiv \frac{1}{\nu_1^{2n+1}}\int_0^{\nu_1}\nu^{2n+1}\text{Im}B^{(-)}(\nu, t)d\nu = \frac{b^-(t)}{\alpha^-(t)+2n+1}\left(\frac{\nu_1}{\nu_0}\right)^{\alpha^-(t)}, \quad (2.8d)$$

where $n = 0, 1, 2, \ldots$ and $\nu_1 \equiv \nu_1(t) = \nu_1(0) + t/4m$, and where

$$\text{Im}A'^{(\pm)}(\nu, t) = \tfrac{1}{2}[\text{Im}A'(\nu, t) \pm \text{Im}\bar{A}'(\nu, t)],$$

$$\text{Im}B^{(\pm)}(\nu, t) = \tfrac{1}{2}[\text{Im}B(\nu, t) \pm \text{Im}\bar{B}(\nu, t)].$$

In principle we evaluate the FESR from knowledge of the low-energy data ($\nu \leq \nu_1$) and calculate the parameters of the leading Regge poles of definite signature, $a^{\pm}(t)$, $b^{\pm}(t)$, and $\alpha^{\pm}(t)$, from

$$\alpha^+(t) = \frac{2nS(B^{(+)}, n) - (2n+2)S(B^{(+)}, n+1)}{S(B^{(+)}, n+1) - S(B^{(+)}, n)}, \quad (2.9a)$$

$$\alpha^-(t) = \frac{(2n+1)S(B^{(-)}, n) - (2n+3)S(B^{(-)}, n+1)}{S(B^{(-)}, n+1) - S(B^{(-)}, n)} \quad (2.9b)$$

and

$$a^+(t) = [\alpha^+(t)+2n+2]S(A'^{(+)}, n)(\nu_1/\nu_0)^{-\alpha^+(t)}, \quad (2.9c)$$

$$a^-(t) = [\alpha^-(t)+2n+1]S(A'^{(-)}, n)(\nu_1/\nu_0)^{-\alpha^-(t)}, \quad (2.9d)$$

$$b^+(t) = [\alpha^+(t)+2n]S(B^{(+)}, n)(\nu_1/\nu_0)^{-\alpha^+(t)}, \quad (2.9e)$$

$$b^-(t) = [\alpha^-(t)+2n+1]S(B^{(-)}, n)(\nu_1/\nu_0)^{-\alpha^-(t)}. \quad (2.9f)$$

The high-energy amplitudes for $K^-n \to \pi^-\Lambda$ and $\pi^+n \to K^+\Lambda$ are then determined from (2.4a) and (2.4b) using the asymptotic expressions for $\hat{A}'^{(\pm)}(\nu, t)$ and $\hat{B}^{(\pm)}(\nu, t)$, (2.6a) and (2.6b):

$$\left.\begin{matrix}A'(\nu, t)\\ \bar{A}'(\nu, t)\end{matrix}\right\} \underset{\nu \text{ large}}{\sim} \left[-a^+(t)\cot\left(\frac{\pi\alpha^+(t)}{2}\right)\left(\frac{\nu}{\nu_0}\right)^{\alpha^+(t)} \pm a^-(t)\tan\left(\frac{\pi\alpha^-(t)}{2}\right)\left(\frac{\nu}{\nu_0}\right)^{\alpha^-(t)}\right] + i\left[a^+(t)\left(\frac{\nu}{\nu_0}\right)^{\alpha^+(t)} \pm a^-(t)\left(\frac{\nu}{\nu_0}\right)^{\alpha^-(t)}\right], \quad (2.10a)$$

$$\left.\begin{matrix}\nu B(\nu,t)\\ \nu\bar{B}(\nu,t)\end{matrix}\right\} \underset{\nu\ \text{large}}{\sim} \left[-b^+(t)\cot\left(\frac{\pi\alpha^+(t)}{2}\right)\left(\frac{\nu}{\nu_0}\right)^{\alpha^+(t)} \pm b^-(t)\tan\left(\frac{\pi\alpha^-(t)}{2}\right)\left(\frac{\nu}{\nu_0}\right)^{\alpha^-(t)}\right] + i\left[b^+(t)\left(\frac{\nu}{\nu_0}\right)^{\alpha^+(t)} \pm b^-(t)\left(\frac{\nu}{\nu_0}\right)^{\alpha^-(t)}\right]. \tag{2.10b}$$

From the above expressions we see that if $\alpha^+(t)=\alpha^-(t)$ (weak EXD) then A' and B are purely real if $a^+(t) = -a^-(t)$ and $b^+(t)=-b^-(t)$, respectively. We refer to this situation as strong EXD.

One can easily express the differential cross section and polarization in terms of A' and B as follows:

$$\frac{d\sigma}{dt}(K^-n\to\pi^-\Lambda)=\left(\frac{1}{64\pi m^2 p_{\text{lab}}{}^2}\right)\left[\frac{(m+m')^4|A'(\nu,t)|^2+\phi(\nu,t)|B(\nu,t)|^2}{(m+m')^2-t}\right], \tag{2.11a}$$

$$P(K^-n\to\pi^-\Lambda)=\frac{2[\phi(\nu,t)]^{1/2}(m+m')^2\operatorname{Im}A'^*B}{(m+m')^4|A'|^2+\phi(\nu,t)|B|^2}. \tag{2.11b}$$

Similar expressions for $(d\sigma/dt)(\pi^+n\to K^+\Lambda)$ and $P(\pi^+n\to K^+\Lambda)$ are obtained by making the substitution $A'\to\bar{A}'$ and $B\to\bar{B}$ in the above formulas. Substituting the high-energy expressions for A' and νB into the formula for the polarization and assuming weak EXD $[\alpha^+(t)=\alpha^-(t)=\alpha(t)]$ yields

$$P(K^-n\to\pi^-\Lambda)=2(m+m')^2[a^-(t)b^+(t)-a^+(t)b^-(t)]\sin[\pi\alpha(t)]\left(\frac{[\phi(\nu,t)]^{1/2}}{\nu}\right)$$
$$\times\left\{(m+m')^4\{[a^+(t)^2+a^-(t)^2]+[a^+(t)^2-a^-(t)^2]\cos[\pi\alpha(t)]\}\right.$$
$$\left.+\frac{\phi(\nu,t)}{\nu^2}\{[b^+(t)^2+b^-(t)^2]+[b^+(t)^2-b^-(t)^2]\cos[\pi\alpha(t)]\}\right\}^{-1},$$

which is energy-independent at large ν [since $(\phi)^{1/2}\sim\nu$]. Thus, if the residues happen to be in the ratio

$$\frac{a^-(t)}{a^+(t)}\approx-\frac{b^-(t)}{b^+(t)}, \tag{2.12}$$

the contributions from the two terms in the numerator reinforce and the polarization becomes large, even if weak EXD is assumed.

B. Evaluation of the Sum Rules, Resonance Parameters, and Poles Below Threshold

There are two major difficulties in attempting a FESR calculation of the high-energy amplitudes. The first is that there exist sizeable unphysical regions in both channels with a number of poles and resonant states whose contributions to the FESR are not experimentally accessible. It will therefore be necessary to use $SU(3)$ estimates of the couplings into those channels for which the resonance is below threshold. The second difficulty is that even above threshold there is no detailed phase-shift information from which to calculate the imaginary parts – all that exist are the parameters of various postulated resonant states whose very existences, let alone couplings, are often debatable.[9] We are therefore forced to make a narrow-resonance approximation for all contributions to the sum rules, whether above or below threshold. This precludes the use of continuous-moment sum rules and means that we will obtain relatively poor information about the effective trajectories.

The individual contributions in the narrow-resonance approximation are derived as follows. For an s-channel resonance the usual Breit-Wigner form yields

$$T_{\text{res}}=\frac{\Phi_s M_s(\Gamma_1\Gamma_2)^{1/2}}{M_s{}^2-s-iM_s\Gamma},$$

where M_s is the mass of the resonance, Γ its total width, Γ_1 and Γ_2 the partial widths $\Sigma^*\to K^-n$ and $\Sigma^*\to\pi^-\Lambda$, respectively, and Φ the relative sign of the resonant amplitude. Similarly for a u-channel resonance we have

$$\bar{T}_{\text{res}}=\frac{\Phi_u M_u(\Gamma_3\Gamma_4)^{1/2}}{M_u{}^2-u-iM_u\Gamma},$$

where Γ_3 and Γ_4 are the partial widths $N^*\to\pi^+n$ and $N^*\to K^+\Lambda$, respectively. Thus in a narrow-resonance approximation we have

$$\operatorname{Im}T_{\text{res}}(\nu,t)=\frac{\pi M_s\Phi_s(\Gamma_1\Gamma_2)^{1/2}}{2m}\delta(\nu-\nu_{\text{res}}),$$

$$\operatorname{Im}\bar{T}_{\text{res}}(\nu,t)=\frac{\pi M_u\Phi_u(\Gamma_3\Gamma_4)^{1/2}}{2m}\delta(\nu-\bar{\nu}_{\text{res}}),$$

where

$$\nu_{\text{res}}=\frac{M_s{}^2-\frac{1}{2}(m^2+m'^2+\mu^2+\mu'^2-t)}{2m}$$

and

$$\bar{\nu}_{\rm res}=\frac{M_u{}^2-\frac{1}{2}(m^2+m'^2+\mu^2+\mu'^2-t)}{2m}.$$

The relationship between ImA and ImB and Im$T_{\rm res}$ follows from

$$\mathrm{Im}A(\nu,t)=K(s)\{C^{(-)}(s)(s^{1/2}+\bar{M})\mathrm{Im}f_1(\nu,t) - C^{(+)}(s)(s^{1/2}-\bar{M})\mathrm{Im}f_2(\nu,t)\},$$

$$\mathrm{Im}B(\nu,t)=K(s)\{C^{(-)}(s)\mathrm{Im}f_1(\nu,t)+C^{(+)}(s)\mathrm{Im}f_2(\nu,t)\},$$

where

$$K(s)=\frac{1}{2s^{1/2}C^{(+)}(s)C^{(-)}(s)}$$

and

$$\bar{M}=\tfrac{1}{2}(m+m'),$$

and where

$$C^{(\pm)}(s)=\frac{1}{8\pi s^{1/2}}[(E_s\pm m)(E'_s\pm m')]^{1/2},$$

TABLE I. Resonance parameters. Spin-parities, masses, total widths, and coupling strengths of resonances entering the sum rules. The sign of each resonant amplitude is given by Φ; $\Gamma_{1,2,3,4}$ are the partial widths for $\Sigma^*\to K^-n$, $\Sigma^*\to\pi^-\Lambda$, $N^*\to\pi^+n$, $N^*\to K^+\Lambda$, respectively. The main entries for each state are the values actually used in the sum rules. The numbers shown in parentheses indicate the range found in different analyses.

Name J^P	M (GeV)	$\Gamma_{\rm tot}$ (GeV)	$10^2\times(\Gamma_1\Gamma_2)^{1/2}$ (GeV)	Φ[a]
		s-channel (Σ^*) resonances		
$\Sigma(1670)\ \frac{3}{2}^-$	1.660 (1.655–1.675)	0.050 (0.04–0.06)	0.5 (0.28–0.66)	−1
$\Sigma(1750)\ \frac{1}{2}^-$	1.730 (1.730–1.764)	0.080 (0.06–0.10)	2.0 (0.9–2.5)	+1
$\Sigma(1765)\ \frac{5}{2}^-$	1.765 (1.755–1.775)	0.100 (0.09–0.125)	2.72 (2.0–3.12)	+1
$\Sigma(1915)\ \frac{5}{2}^+$	1.895 (1.885–1.935)	0.070 (0.027–0.090)	0.49 (0.27–1.26)	+1
$\Sigma(1920)\ \frac{1}{2}^+$	1.920 (1.900–2.000)	0.170 (0.130–0.250)	2.38 (1.43–3.56)	+1
$\Sigma(1940)\ \frac{3}{2}^-$	1.940 (1.890–1.990)	0.280 (0.15–0.32)	3.92 (1.2–5.45)	+1
$\Sigma(2030)\ \frac{7}{2}^+$	2.022 (1.995–2.040)	0.170 (0.100–0.195)	3.4 (2.59–4.28)	−1
$\Sigma(2080)\ \frac{3}{2}^+$	2.070 (2.040–2.120)	0.250 (0.067–0.290)	2.25 (0.87–3.48)	+1
		u-channel (N^*) resonances		
$N(1675)\ \frac{5}{2}^-$	1.680 (1.655–1.680)	0.170 (0.105–0.175)	0.18 (<0.3)	−1[b]
$N(1688)\ \frac{5}{2}^+$	1.690 (1.680–1.692)	0.130 (0.105–0.180)	0.10 (<0.3)	−1[b]
$N(1700)\ \frac{1}{2}^-$	1.710 (1.665–1.765)	0.300 (0.100–0.400)	3.4 (2.0–3.4)	−1
$N(1780)\ \frac{1}{2}^+$	1.751 (1.640–1.860)	0.227 (0.160–0.450)	1.1 (1.1–4.0)	+1
$N(1860)\ \frac{3}{2}^+$	1.863 (1.840–1.900)	0.296 (0.220–0.450)	1.48 (1.1–3.34)	−1

[a] For those resonances listed in Table 3 of Levi-Setti (Ref. 22) our phases Φ are uniformly of opposite signs from those determined from Levi-Setti's $SU(3)$ sign of the resonant amplitude times the phase of the $SU(2)$ Clebsch-Gordan coefficient (using his stated convention of the ordering of the baryon and meson). This over-all sign difference is obviously of no consequence; it arises from different choices of signs for the isospin states for π^+ relative to π^- and K^- relative to K^+ more appropriate in s-u crossing.

[b] The $N(1675)$ and $N(1688)$ couple very weakly, if at all, to the $K^+\Lambda$ channel. Their presence has little effect on the high-energy differential cross section at small t, but the indicated small amounts improve the behavior at $|t|>0.5$ $(\mathrm{GeV}/c)^2$.

$$\mathrm{Im}f_1(\nu,t)=\sum_{l=0}^{\infty}[\mathrm{Im}f_{l+}(s^{1/2})P_{l+1}'(\cos\theta_s)$$
$$-\mathrm{Im}f_{l-}(s^{1/2})P_{l-1}'(\cos\theta_s)],$$
$$\mathrm{Im}f_2(\nu,t)=\sum_{l=0}^{\infty}[\mathrm{Im}f_{l-}(s^{1/2})$$
$$-\mathrm{Im}f_{l+}(s^{1/2})]P_l'(\cos\theta_s).$$

Keeping track of the normalization, one finds

$$\mathrm{Im}f_{l\pm}(\nu,t)=\frac{1}{(p_s p_s')^{1/2}}\mathrm{Im}T_{\mathrm{res}}.$$

Similar expressions for $\mathrm{Im}\bar{A}$ and $\mathrm{Im}\bar{B}$ in terms of $\mathrm{Im}\bar{T}_{\mathrm{res}}$ are obtained by substituting $s\to u$, $\cos\theta_s \to \cos\theta_u$, $E_s\to E_u$, $E_s'\to E_u'$ in the above expressions and using

$$\mathrm{Im}\bar{f}_{l\pm}(\nu,t)=\frac{1}{(p_u p_u')^{1/2}}\mathrm{Im}\bar{T}_{\mathrm{res}}.$$

We use the $Y=0$ s-channel resonances (Σ^*'s) to form the amplitudes $\mathrm{Im}A$ and $\mathrm{Im}B$ and the $Y=1$ u-channel resonances (N^*'s) to form the amplitudes $\mathrm{Im}\bar{A}$ and $\mathrm{Im}\bar{B}$, leading eventually to the representation of the sum rules (2.8) as sums over the s- and u-channel poles. In Table I we list the parameters of the resonant amplitudes for the s- and u-channel states considered in this study. There are a number of independent analyses of both $K^-n\to\pi^-\Lambda$ (Refs. 9–14) and $\pi^+n\to K^+\Lambda$ (Refs. 15–17), yielding somewhat different parametrizations and even different numbers of resonances. The ranges of parameters found in these analyses, and also from the compilation of the Particle Data Group,[18] are shown in Table I in addition to the values used by us. As pointed out by Galtieri,[9] there is agreement among the various analyses of $K^-n\to\pi^-\Lambda$ only for the three resonances $\Sigma(1765)\ \frac{5}{2}^-$, $\Sigma(1915)\ \frac{5}{2}^+$, and $\Sigma(2030)\ \frac{7}{2}^+$. The remaining five Σ states in Table I are controversial. Tests were made of the sensitivity of the sum rules to our particular choice of parameters. While some changes occur when other possible sets of resonance parameters are used, the effects are in general not marked.

From the point of view of fitting the high-energy differential cross section for $K^-n\to\pi^-\Lambda$, there is, however, some difficulty caused by the $\Sigma(1940)\ \frac{3}{2}^-$ state *if* all the resonance parameters of Table I (our specific choices) are employed. This state, reported by Litchfield[10] and Galtieri,[9] is important enough that its presence or absence has a significant effect on the high-energy observables. When the present work was begun this state was sufficiently doubtful that we felt justified in omitting it from the analysis. All the curves given below are calculated with the parameters of Table I, except for the omission of the $\Sigma(1940)\ \frac{3}{2}^-$. During the preparation of this paper we have become persuaded that this resonance is at least as real as some of the others [e.g., $\Sigma(2080)\ \frac{3}{2}^+$], and have therefore reexamined its inclusion. We are able to obtain almost the same Regge parameters and fit at high energies with modest changes of the parameters of some of the other states in Table I (always within the limits of error listed in Table III of Galtieri[9]). At the appropriate place below we indicate the small changes that occur in the Regge parameters for this revision of the low-energy sums.

There are six "pole" terms that lie below threshold; the $N(938)\ \frac{1}{2}^+$, $N(1470)\ \frac{1}{2}^+$, $N(1518)\ \frac{3}{2}^-$, and $N(1550)\ \frac{1}{2}^-$ in the u channel; and the $\Sigma(1197)\ \frac{1}{2}^+$ and $\Sigma(1385)\ \frac{3}{2}^+$ in the s channel. We use the Lagrangians shown in Table II to calculate these pole terms. The contributions to $\mathrm{Im}A$, etc. are shown in Table III in terms of kinematic variables and products of couplings appropriate to the charge states involved. We now proceed to estimate these coupling constants, using the following values for the widths:

$$\Gamma(N^+(1470)\to\pi^0 p)=40\ \mathrm{MeV},$$
$$\Gamma(N^+(1518)\to\pi^0 p)=20\ \mathrm{MeV},$$
$$\Gamma(N^+(1550)\to\pi^0 p)=9\ \mathrm{MeV}.$$

These specific values are rather arbitrary, but the

TABLE II. Widths for the decay of a baryon a of mass M and spin-parity J^P into a $\frac{1}{2}^+$ baryon b of mass m and a 0^- meson of mass μ, and the Lagrangians used in calculating the widths. (The symbols p and E are the c.m. momentum and energy, respectively, of the final baryon.)

J^P	Lagrangian	Width Γ
$\frac{1}{2}^-$	$g\bar{\psi}_b(x)\psi_a(x)\phi^\dagger(x)+\mathrm{H.c.}$	$(g^2/8\pi M^2)[(M+m)^2-\mu^2]p$
$\frac{1}{2}^+$	$-ig\bar{\psi}_b(x)\gamma_5\psi_a(x)\phi^\dagger(x)+\mathrm{H.c.}$	$(g^2/4\pi)[M(E+m)]^{-1}p^3$
$\frac{3}{2}^+$	$g\left(\frac{\partial\bar{\psi}_b(x)}{\partial x_\alpha}\Phi_\alpha^a(x)\right)\phi^\dagger(x)+\mathrm{H.c.}$	$(g^2/24\pi\mu^2M^2)[(M+m)^2-\mu^2]p^3$
$\frac{3}{2}^-$	$ig\left(\frac{\partial\bar{\psi}_b(x)}{\partial x_\alpha}\gamma_5\Phi_\alpha^a(x)\right)\phi^\dagger(x)+\mathrm{H.c.}$	$(g^2/12\pi\mu^2)[M(E+m)]^{-1}p^5$

TABLE III. Pole-term contributions to ImA, ImB, Im$\bar{A}$, and Im$\bar{B}$.

J^P	Pole-term contributions
	s channel
$\frac{1}{2}^+$	$\mathrm{Im}A(\nu,t) = -\pi(g_{N\bar{K}\Sigma^*} g_{\Sigma^*\Lambda\pi}/4m)(2M_{\Sigma^*} - m - m')\delta(\nu - \nu_{\Sigma^*})$
	$\mathrm{Im}B(\nu,t) = \pi(g_{N\bar{K}\Sigma^*} g_{\Sigma^*\Lambda\pi}/2m)\delta(\nu - \nu_{\Sigma^*})$
$\frac{3}{2}^+$	$\mathrm{Im}A(\nu,t) = \pi(g_{N\bar{K}\Sigma^*} g_{\Sigma^*\Lambda\pi}/6m\mu\mu')\{3[M_{\Sigma^*} + \frac{1}{2}(m+m')]p_s p_s' \cos\theta_s + [M_{\Sigma^*} - \frac{1}{2}(m+m')](E_s + m)(E_s' + m')\}\delta(\nu - \nu_{\Sigma^*})$
	$\mathrm{Im}B(\nu,t) = \pi(g_{N\bar{K}\Sigma^*} g_{\Sigma^*\Lambda\pi}/6m\mu\mu')[3p_s p_s' \cos\theta_s - (E_s + m)(E_s' + m')]\delta(\nu - \nu_{\Sigma^*})$
	u channel
$\frac{1}{2}^+$	$\mathrm{Im}\bar{A}(\nu,t) = -\pi(g_{N\pi N^*} g_{N^*\Lambda K}/4m)(2M_{N^*} - m - m')\delta(\nu - \bar{\nu}_{N^*})$
	$\mathrm{Im}\bar{B}(\nu,t) = \pi(g_{N\pi N^*} g_{N^*\Lambda K}/2m)\delta(\nu - \bar{\nu}_{N^*})$
$\frac{1}{2}^-$	$\mathrm{Im}\bar{A}(\nu,t) = \pi(g_{N\pi N^*} g_{N^*\Lambda K}/4m)(2M_{N^*} + m + m')\delta(\nu - \bar{\nu}_{N^*})$
	$\mathrm{Im}\bar{B}(\nu,t) = \pi(g_{N\pi N^*} g_{N^*\Lambda K}/2m)\delta(\nu - \bar{\nu}_{N^*})$
$\frac{3}{2}^-$	$\mathrm{Im}\bar{A}(\nu,t) = \pi(g_{N\pi N^*} g_{N^*\Lambda K}/6m\mu\mu')\{3[-M_{N^*} + \frac{1}{2}(m+m')]p_u p_u' \cos\theta_u - [M_{N^*} + \frac{1}{2}(m+m')](E_u - m)(E_u' - m')\}\delta(\nu - \bar{\nu}_{N^*})$
	$\mathrm{Im}\bar{B}(\nu,t) = \pi(g_{N\pi N^*} g_{N^*\Lambda K}/6m\mu\mu')\{3p_u p_u' \cos\theta_u - (E_u - m)(E_u' - m')\}\delta(\nu - \bar{\nu}_{N^*})$

widths of these resonances are quite uncertain. Our choices are within the allowed ranges quoted by the Particle Data Group.[18] When we use the formulas of Table II the coupling constants in the effective Lagrangians are found to be

$$g(N^+(1470) \to \pi^0 p) = 4.5,$$

$$(1/\mu)g(N^+(1518) \to \pi^0 p) = 10.8,$$

$$g(N^+(1550) \to \pi^0 p) = 0.4.$$

Assuming each to be a member of an $SU(3)$ octet with the $D/(F+D)$ ratio given in Table IV, we use $SU(3)$ to determine the unobservable coupling constants,

$$g(N^+(1470) \to K^+\Lambda) = -4.6,$$

$$(1/\mu)g(N^+(1518) \to K^+\Lambda) = -11.6,$$

$$g(N^+(1550) \to K^+\Lambda) = 0.2.$$

Similarly, using

$$\Gamma(\Sigma^-(1385) \to \pi^-\Lambda) = 32.4 \text{ MeV}$$

and Table II, we obtain

$$(1/\mu)g(\Sigma^-(1385) \to \pi^-\Lambda) = 9.1.$$

With exact $SU(3)$ for the decuplet, the $\Sigma^-(1385) \to K^- n$ coupling is

$$(1/\mu)g(\Sigma^-(1385) \to K^- n) = -(\tfrac{2}{3})^{1/2}(9.1) = -7.4.$$

If we had begun instead with the width of 120 MeV for the $\Delta(1238)$, these values of 9.1 and −7.4

TABLE IV. Poles lying below threshold.

Name	Mass (MeV)	$SU(3)$ multiplet	$D/(D+F)$	Reference
		s channel		
$\Sigma(1197)\ \frac{1}{2}^+$	1197	octet	0.6	canonical value
$\Sigma(1385)\ \frac{3}{2}^+$	1385	decuplet	⋯	
		u channel		
$N(938)\ \frac{1}{2}^+$	938	octet	0.6	canonical value
$N(1470)\ \frac{1}{2}^+$	1470	octet	0.6	a
$N(1518)\ \frac{3}{2}^-$	1520	octet	0.565	Levi-Setti[b]
$N(1550)\ \frac{1}{2}^-$	1535	octet	1.96	Levi-Setti[b]

[a] We estimated this from the decays $N(1470) \to N\pi$ and $N(1470) \to N\eta$.

[b] Reference 22.

would have been 10.9 and −8.9, respectively. This gives some indication of the magnitude of the symmetry breaking for the $\frac{3}{2}^+$ decuplet. Warnock and Frye's values[19] of the $\Sigma^-(1385) \to K^- n$ coupling constant are equivalent in our notation to −8.3 [exact $SU(3)$, $\Delta(1238)$ width] and −7.4 [broken $SU(3)$]. It happens that our first estimate is numerically the same as Warnock and Frye's preferred value.[19]

The relevant N and Σ coupling constants are shown in Fig. 4 as a function of $D/(D+F)$, assuming exact $SU(3)$ symmetry and $g(p \to \pi^0 p) = 13.55$. The early empirical determinations of Zovko[20] and Kim,[21] shown in the figure, indicate that $D/(D+F)$ is in the range 0.5–0.8, but also imply some symmetry breaking. Numerous other estimates of the $\Sigma\bar{K}N$ and $\Lambda\bar{K}N$ couplings have been made. As can be seen from Fig. 27 of Levi-Setti,[22] the $\Lambda\bar{K}N$ values cluster around either Kim's of Zovko's value, with no clear preference indicated. The square of the $\Sigma\bar{K}N$ coupling constant is always found to be small, with Zovko's value as a rough upper limit. Also shown in Fig. 4 is the estimate for $g(\Sigma^0 \to \pi^0 \Lambda)$ of Chan and Meiere.[23] Our calculation involves the products $g(\Sigma^- \to K^- n) g(\Sigma^0 \to \pi^0 \Lambda)$ for the $\Sigma(1197)$ pole and $g(p \to \pi^0 p) g(p \to K^+ \Lambda)$ for the $N(938)$ pole, with appropriate isospin coefficients.

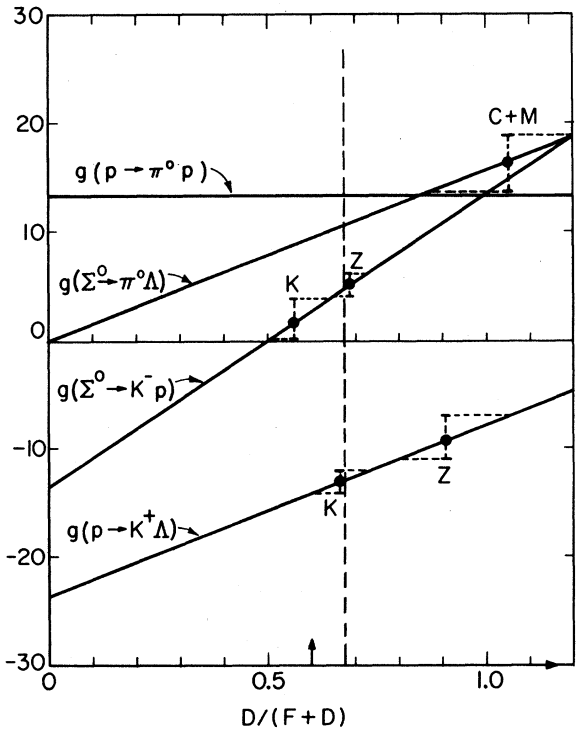

FIG. 4. $SU(3)$ coupling constants for the pseudoscalar meson-baryon-baryon vertices of the $\frac{1}{2}^+$ baryon octet as a function of $D/(D+F)$. The πNN coupling constant is defined by $g^2/4\pi = 14.6$, corresponding to $g(p \to \pi^0 p) = 13.55$. The points with "errors" indicate ranges of the indicated coupling constants found by Kim (K), Ref. 21, Zovko (Z), Ref. 20, and Chan and Meiere (C+M), Ref. 23. The arrow indicates the canonical theoretical value of $D/(D+F) = 0.6$; the dashed line at 0.675 is our preferred value.

C. Sensitivity to the Couplings of the Pole Terms

It is painfully obvious that there is tremendous latitude in the specific choice of coupling constants for the states below threshold. Some states, such as the $N(1470)$, $N(1518)$, and $N(1550)$, are relatively unimportant in the sum rules. Variation of their couplings around the values given above produces no major effects. For the $\frac{1}{2}^+$ baryon octet poles and the $\Sigma(1385)$, however, the contributions are of sufficient importance that the results are sensitive to the exact values of the couplings. Numerous exploratory calculations were made to study these variations. Even though the exact use of the sum rules and the assumptions made in determining the trajectories and residues are not de-

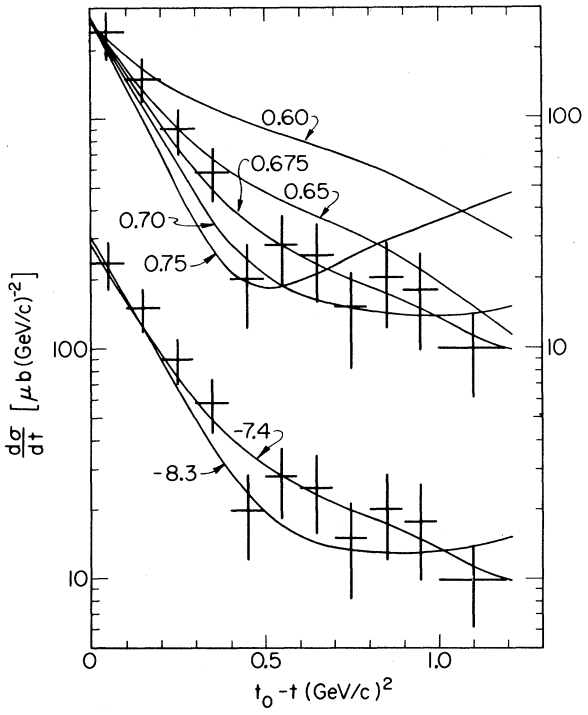

FIG. 5. Effects of variation of coupling constants on the high-energy differential cross section for $K^- n \to \pi^- \Lambda$. The data shown are those of Yen *et al.*[4] at 4.5 GeV/c. The upper curves (ordinate scale on the right) show the effects of varying the $D/(D+F)$ ratio for the $N(938)$ and $\Sigma(1197)$ pole terms. The numbers beside the curves are the values of $D/(D+F)$. The lower curves (ordinate scale on the left) show the effects of different $\Sigma^-(1385) \to K^- n$ couplings, with $D/(D+F) = 0.675$ for N and Σ poles and the other resonance parameters fixed from experiment. The numbers beside the curves are values of $\mu^{-1} g(\Sigma^-(1385) \to K^- n)$.

scribed until the next section, Sec. III, we illustrate in Fig. 5 the effect on the differential cross section at high energies. In the upper half of the figure the change produced by variation of the $D/(D+F)$ ratio of the $\frac{1}{2}^+$ octet is shown, all other couplings being held fixed. The curves are for different ratios $D/(D+F)$ assuming exact $SU(3)$ for all vertices, but similar variations occur if random combinations of Kim's and Zovko's values are chosen. If the couplings are forced to be $SU(3)$ symmetric, the optimum $D/(D+F)$ ratio is in the range 0.65–0.70,[24] not far from the canonical value of 0.6. The lower half of Fig. 5 shows the effect of varying the coupling of the $\Sigma(1385)$. The two curves are for the exact and broken $SU(3)$ estimates of Warnock and Frye for the coupling to the $\bar{K}N$ channel quoted above, the coupling to the $\pi\Lambda$ channel being fixed from experiment. The $\Sigma(1197)$ and $N(938)$ pole contributions are fixed by $D/(D+F) = 0.675$. The experimental cross sections at high energy slightly favor the value $(1/\mu)g(\Sigma^-(1385) \to K^-n) = -7.4$. There is evidently some possibility of trading off changes in the $\frac{1}{2}^+$ octet couplings against changes in the $\Sigma(1385)$ coupling. Our choices of $D/(D+F)$ for the $\frac{1}{2}^+$ octet and couplings for the $\Sigma(1385)$ are certainly in the comfortable range of expected values, but are in no way unique. The results are most sensitive to the value of $D/(D+F)$. A value outside the range of 0.6 to 0.7 [or its equivalent for broken $SU(3)$] leads to a bad fit to the high-energy observables for $K^-n \to \pi^-\Lambda$. The $\Sigma(1385)$ couplings are less crucial, but cannot be varied by more than 20% without serious difficulty.

III. RESULTS

A. Trajectories, High-Energy Cross Sections, and Polarization

As is perhaps apparent from Sec. II, the uncertainties of the couplings and the necessity of making a narrow-resonance approximation preclude the use of anything but the lowest moment ($n=0$) sum rules. We are thus unable to calculate the Regge trajectories $\alpha^{\pm}(t)$ from the formulas (2.9a) and (2.9b). We assume that the trajectories have unit slope (1 GeV^{-2}) and determine the intercepts in the following way. The even-signatured residues $a^+(t)$ and $b^+(t)$ must vanish at the right-signature point, $\alpha^+(t)=0$, in order that the real parts of the amplitudes not be singular in the physical region. From (2.9e) it can be seen that the $n=0$ sum rule for $b^+(t)$ automatically satisfies this requirement. For $a^+(t)$, however, (2.9c) shows that we must define $\alpha^+(t)=0$ at the t value where $S(A'^{(+)}, 0)=0$.[25] The trajectory $\alpha^+(t)$ is thereby determined. For the odd-signatured amplitudes we appeal to the presence of a sense-nonsense factor of $\alpha^-(t)$ in the residue $b^-(t)$. From (2.9f) it is seen that $\alpha^-(t)=0$ is then defined as the t value where $S(B^{(-)}, 0)=0$. The question of whether $b^-(t)$ has additional factors of $\alpha^-(t)$ is left open, to be answered by the sum rules themselves. It should be remarked that the vanishing of $S(B^{(-)}, 0)$ can be attributed to interference between Regge-pole and Regge-cut amplitudes, rather than to the presence of a factor of $\alpha^-(t)$ in a purely Regge-pole amplitude. Because of our limitation in the sum rules to two effective Regge poles, one for each signature, we cannot speak on this point. We merely assume that the vanishing of the effective residue $b^-(t)$ signifies $\alpha^-(t)=0$.

The residues $a^+(t)$, $a^-(t)$, $b^+(t)$, $b^-(t)$ are calculated from Eqs. (2.9c)–(2.9f) with $n=0$, the trajectories having been found as described above. The exact values of the *residues* depend on the upper limit ν_1 in the sum rules and on the choice of $\nu_0 \equiv s_0/2m$.[26] We take $s_0=1$ GeV and use $\nu_1(t) = \nu_1(0) + t/4m$, with $\nu_1(0)$ slightly above the highest-mass resonance included in the sum rule. The standard value employed is $\nu_1(0)=1.8$, corresponding to $M=2.14$ GeV. The results are insensitive to changes of 10% in $\nu_1(0)$. If $\nu_1(0)$ is lowered below the highest Σ resonance in Table I and its contribution is therefore omitted, the two zeros of $S(A'^{(+)}, 0)$ just disappear. [The inverted parabola for $a^+(t)$ of Fig. 10 drops below the axis.] This

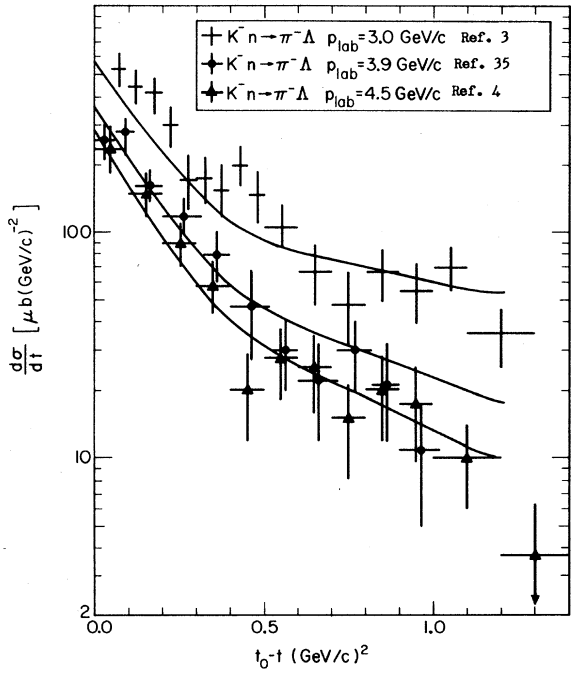

FIG. 6. Comparison of calculated and experimental differential cross sections for $K^-n \to \pi^-\Lambda$ at 3.0, 3.9, and 4.5 GeV/c.

means that α^+ cannot be defined as before and also that the real part of the Regge-pole amplitude has a pole in the physical region, or else there is a 0^+ particle of small mass. Nevertheless, the high-energy observables are changed very little, except in the immediate vicinity of the spurious pole. Furthermore, small changes in the resonance parameters can bring back the two zeros in $S(A'^{(+)}, 0)$. Similarly, inclusion of the $\Sigma(2060)\frac{7}{2}^-$ of Galtieri[9] (not listed in Table I) changes the observables only slightly. We conclude that our sum rules are reasonably insensitive to the detailed behavior at the upper limit ν_1.

As already described in Sec. II C, the Σ and N pole terms are very important in the sum rules and the $\Sigma(1385)$ somewhat less so. The $D/(D+F)$ ratio of the $\frac{1}{2}^+$ octet was therefore varied to optimize the fit to the data on the differential cross section for $K^-n \to \pi^-\Lambda$, as shown above in Fig. 5. The "best" solution $[D/(D+F) = 0.675]$ is compared with the experimental cross sections for $K^-n \to \pi^-\Lambda$ at 3.0, 3.9, and 4.5 GeV/c in Fig. 6. In Fig. 7 we show the polarization resulting from our solution and the corresponding data at 3.0 and 4.5 GeV/c (Refs. 3 and 4, respectively), and in Fig. 8 we display our predictions for the A and R parameters of Wolfenstein[27] at 4.5 and 9 GeV/c. Our polarization and A and R parameters are essentially independent of energy. In Fig. 9 we compare our prediction for the slope parameter b ($d\sigma/dt \simeq Ae^{bt}$) with the results of experiment at various momenta. These figures show that our solution is in good agreement with existing differential cross sections for $K^-n \to \pi^-\Lambda$, gives an energy variation and magnitude of b consistent with the data, including recent results from SLAC,[28] and is in agreement with the rather inaccurate data on polarization for $0 < |t| < 1.0$.

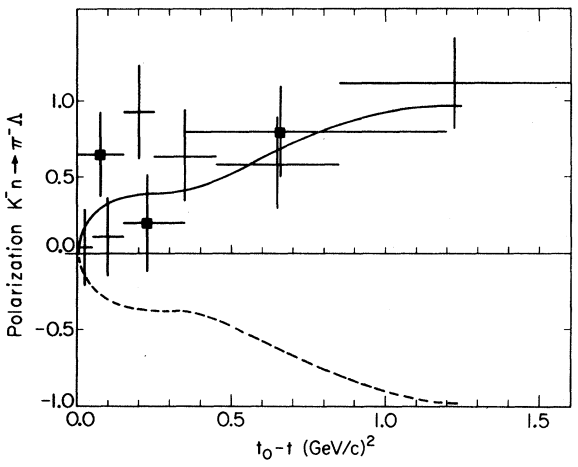

FIG. 7. Comparison of calculated and experimental Λ polarization for $K^-n \to \pi^-\Lambda$. Solid squares are the data of Yen *et al.*[4] at 4.5 GeV/c. Crosses are the data of Barloutaud *et al.*[3] at 3.0 GeV/c. The solid (dashed) curve is for $K^-n \to \pi^-\Lambda$ ($\pi^+n \to K^+\Lambda$) and is essentially energy-independent.

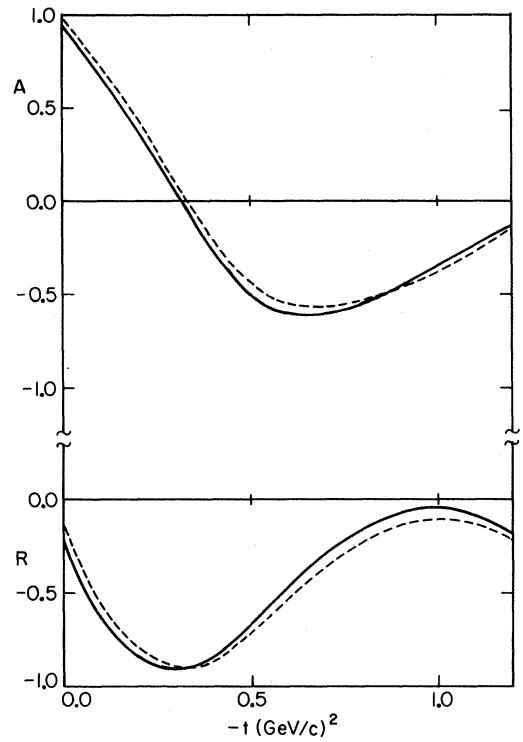

FIG. 8. Predictions of the A and R parameters for $K^-n \to \pi^-\Lambda$ at 4.5 GeV/c (solid curve) and 9 GeV/c (dashed curve).

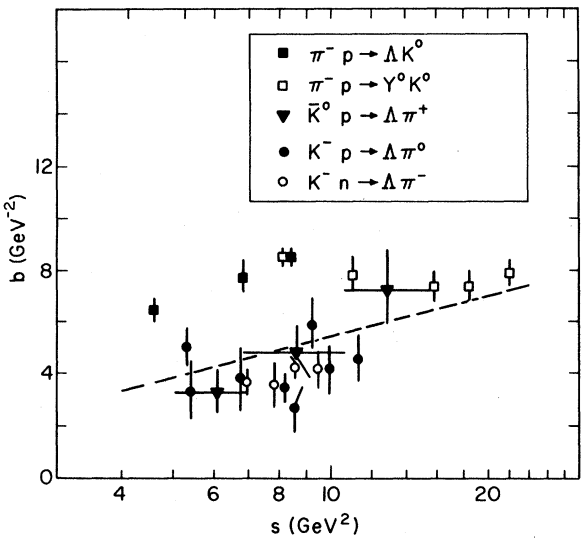

FIG. 9. Slope parameters of $d\sigma/dt$ versus s. Same as Fig. 7 of Lai and Louie (Ref. 5), but with the SLAC results (Ref. 28) (solid triangles) and our calculated slope for $K^-n \to \pi^-\Lambda$ (dashed curve) added. References for the remaining data are found in Table 3 of Ref. 5.

Comparison of our solution with the line-reversed process, $\pi^+ n \to K^+ \Lambda$, is deferred until after a discussion of the residues themselves and questions of exchange degeneracy.

B. Residues, Exchange Degeneracy, and Duality

The residues $a^{\pm}(t)$ and $b^{\pm}(t)$ for the "best" solution are shown in Fig. 10. The residues $a^+(t)$ and $b^-(t)$ vanish at $t=-0.15$ and $t=-0.18$, respectively, corresponding to trajectories $\alpha^+(t)=0.15+t$ and $\alpha^-(t)=0.18+t$. Our solution thus exhibits approximate weak EXD. The t-channel spin-flip residues $b^{\pm}(t)$ are seen to satisfy the relation $b^{\pm}(t)\approx -b^-(t)$ over a large range of t. This is evidence for strong EXD for the spin-flip residues. The t-channel nonflip residues $a^+(t)$ and $-a^-(t)$ have the same general shape, but differ by a low-order polynomial. Evidently strong EXD does not hold for the nonflip residues.[29] It is of interest, nevertheless, to display the degree of exchange degeneracy in the amplitudes in another manner in order to understand better how well or how badly EXD is satisfied. From EXD arguments or duality diagrams, we expect the amplitudes (A', B) for $K^-n \to \pi^-\Lambda$ to be real, while the amplitudes $(\bar{A}', \bar{B})$ for $\pi^+n \to K^+\Lambda$ should have a t-dependent phase factor, $\exp[-i\pi\alpha(t)]$. In Fig. 11 are displayed the phases of A', B, $\bar{A}'$, and $\bar{B}$ as functions of $-t$. The strikingly different t dependences of the phases for (A', B) and $(\bar{A}', \bar{B})$ are apparent. Furthermore, the phases of A' and B are small for $|t|<0.5$, especially that of B. Now, a t-independent phase for A' of only 20° and a much smaller phase for B can plausibly be argued as evidence for reasonable exchange degeneracy and a vindication of duality diagrams. Nevertheless, this relatively modest phase difference between A' and B is responsible for the nonvanishing polarization shown in Fig. 7.[30] This emphasizes once again that polarizations are delicate quantities and that yes-no theoretical predictions about them are hazardous. Conversely, it argues against judging the *over-all* success of a model or theoretical principle by how well it does in predicting polarization.

For those readers who prefer to consider s-

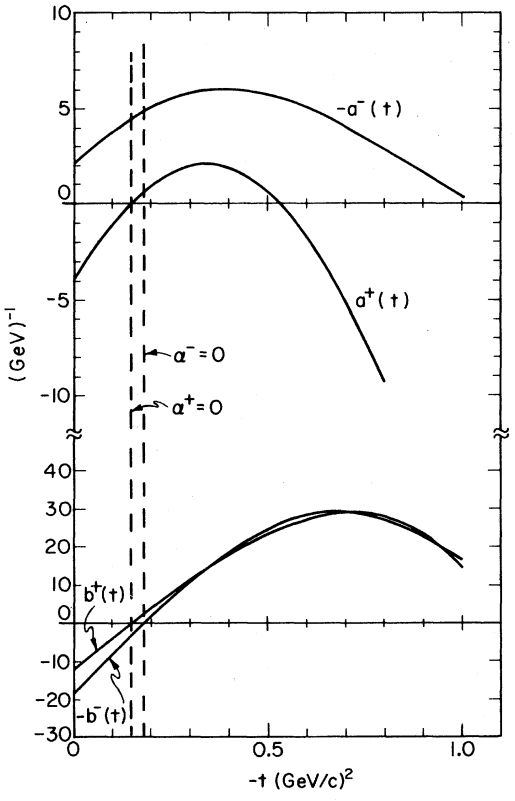

FIG. 10. Regge residues $a^{\pm}(t)$, $b^{\pm}(t)$ of the t-channel nonflip and flip amplitudes, respectively, as functions of t. The zeros of a^+ and b^- define the vanishings of the trajectories α^+ and α^-, as indicated by the vertical dashed lines. Exact exchange degeneracy implies $a^+=-a^-$, $b^+=-b^-$.

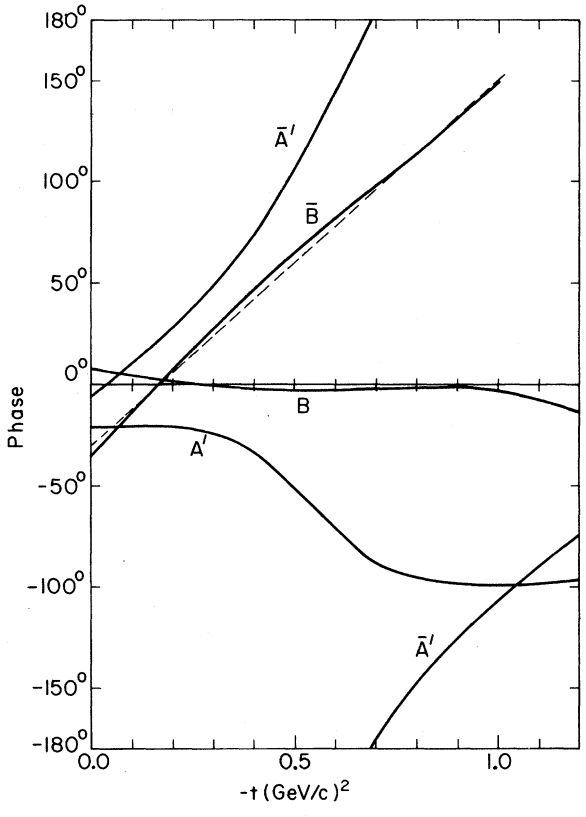

FIG. 11. Phases of the high-energy amplitudes A' and B for $K^-n \to \pi^-\Lambda$, and $\bar{A}'$ and $\bar{B}$ for $\pi^+n \to K^+\Lambda$ as functions of t. Duality diagrams predict zero phase for A' and B, and a phase $-\pi\alpha(t)$ for $\bar{A}'$ and $\bar{B}$. The dashed line gives the average phase, $-\pi[\alpha^+(t)+\alpha^-(t)]/2$, for comparison.

channel helicity amplitudes, we remark that for the process $K^-n \to \pi^-\Lambda$ the t dependences of the real parts of the s-channel amplitudes H_{++} and H_{+-} are qualitatively similar to those shown in Figs. 1(b) and 1(d) of Berger and Fox,[27] although the relative signs are opposite from what is shown there. The imaginary part of H_{+-} is very small and roughly constant in t, while the ratio of imaginary to real part of H_{++} is -0.3 at $t=0$ and increases (in magnitude) smoothly to roughly -1 at $t \simeq -1.0$ (GeV/c)^2.

In Sec. II B we noted that some of the resonances in Table I were controversial, and that we had omitted the $\Sigma(1940)\ \frac{3}{2}^-$ state from the sum rules. A fit is still possible with this state included, provided some of the widths are altered. One fit that yields $\alpha^+ = 0.14 + t$, $\alpha^- = 0.24 + t$, and residues almost identical with those of Fig. 10 has the couplings of Table I modified to $(\Gamma_1\Gamma_2)^{1/2} = 2.0\times10^{-2}$, 1.2×10^{-2}, 3.6×10^{-2}, for the 1765, 1940, 2030 states, respectively. The observables from this solution are almost identical with those of Figs. 6, 7, and 8.

Another aspect of the residues shown in Fig. 10 is the degree of correlation between the zeros of the residues and the zeros of the contributions to the various sum rules from the individual resonances. It is well known that such correlations formed the original motivation for the concept of duality.[31] The zeros of the various contributions to ImA' and ImB are shown in Fig. 12. First consider the zero in $a^+(t)$ at $t \approx -0.15$ (GeV/c)^2. From Fig. 12 it is seen that the important contributors to $a^+(t)$ have zeros at small t, clustered in fact quite closely around $t=-0.15$. The only important exceptions appear to be the $\Sigma(1197)$ and $N(938)$. The sum rule for $a^+(t)$ involves Im$(\nu A'^{(+)})$, however, and the values of ν for the $\Sigma(1197)$ and $N(938)$ are so small that their contributions are unimportant over the whole range of $|t|<0.5$. Within the framework of two effective Regge poles at high energy it is gratifying that for the even-signatured amplitude the resonances individually give zeros where $a^+(t) = 0$ and $\alpha^+(t) = 0$. The avoidance of a "ghost pole" at negative t is apparently sufficiently important not to be left to chance cancellations in the sum rule.

For $a^-(t)$ the sum rule involves Im$(A'^{(-)})$. The $\Sigma(1197)$ and the $N(938)$ contributions are no longer suppressed. This is one of the major reasons for the difference between $a^+(t)$ and $-a^-(t)$ seen in Fig. 10. From Fig. 12 it is evident that the zero in $b^-(t)$ at $t=-0.18$ (GeV/c)^2 is not produced by a zero from each resonance, but rather by a cumulative cancellation in the sum rule. Such behavior is in contrast with that found originally by Dolen, Horn, and Schmid[31] for the ρ Regge pole in πN elastic scattering. The present mechanism for generating a zero in $b^-(t)$ arises because of the alternations in sign caused by the approximate EXD of the s-channel resonances, as discussed immediately below.

The discussion thus far has concerned EXD or lack of it for the K^* and K^{**} trajectories and residues. The same duality diagrams of Fig. 1 that predict EXD for the K^* and K^{**} also show that the s-channel resonances are generated only by u-channel exchanges. This implies that the predominant Σ^* resonances which enter our sum rules should also lie on trajectories occurring in EXD pairs and have residues equal in magnitude, but opposite in sign. A test of this hypothesis is shown in Fig. 13, where the relevant baryon trajectories are displayed, as well as the contributions to the sum rule for ImB at $t=m_{K^*}{}^2$.[32] The dominant Σ^* resonances do seem to be roughly EXD, lying closely on two trajectories rather than four. The contributions from successive resonances on a single EXD pair of trajectories alternate in sign, and the absolute values have a smooth variation with mass. The cancellation of s-channel imaginary parts shown in Fig. 13 was previously tested by Ferro-Luzzi *et al.*[33] with experimental data on the amplitudes for the mass interval 2.25 GeV$^2 \leq s \leq$ 3.61 GeV^2. This analysis argued against semilocal duality in the sense of cancellations, but as is indicated on Fig. 13, the mass interval is such that only *one* important resonance from each pair of trajectories contributes. It happens that these two resonances do not cancel; the cancellation comes from successive members of each EXD sequence. The N^* states in the u channel are not expected to be exchange-degenerate in their couplings, and they do not seem to be so.

To conclude this discussion of residues and

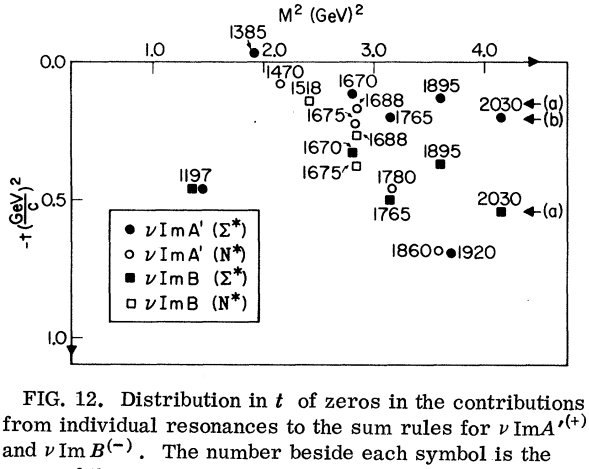

FIG. 12. Distribution in t of zeros in the contributions from individual resonances to the sum rules for $\nu\,\mathrm{Im}A'^{(+)}$ and $\nu\,\mathrm{Im}\,B^{(-)}$. The number beside each symbol is the mass of the resonance. The arrows on the right indicate the zeros in the $A'^{(+)}$ sum rule (a) and the $B^{(-)}$ sum rule (b). The contributions to the $A'^{(+)}$ sum rule from the $N^*(1780)$, $N^*(1860)$, and $\Sigma^*(1920)$, with zeros near $t=-0.5$, are relatively unimportant.

couplings we comment briefly on the "sense-choosing" and "ghost-eliminating" mechanisms[34] for the K^* and K^{**} Regge poles, or more precisely, on the type of zeros occurring in the residues of the effective poles. From Fig. 10 it can be seen that the K^{**} appears to choose the Gell-Mann mechanism with a dynamical zero in the $A'^{(+)}$ residue at larger $|t|$, while the K^* chooses sense. The behavior of the even-signature residue is similar to that reported for the P' and A_2 trajectories, although there is still some argument about the latter. Arguments on $SU(3)$ grounds would tend to favor similar mechanisms for P', A_2, and K^{**}, and similarly for the K^* and ρ.

C. Troubles: $\pi^+ n \to K^+ \Lambda$

We have thus far discussed only the successes of our sum-rule calculation. We must now illustrate some of its glaring failures. Our solution exhibits approximate weak EXD $[\alpha^+(t) \approx \alpha^-(t)]$. Independent of the residues, we thus predict

$$\frac{d\bar{\sigma}}{dt} \approx \frac{d\sigma}{dt}$$

and

$$\bar{P} \approx -P$$

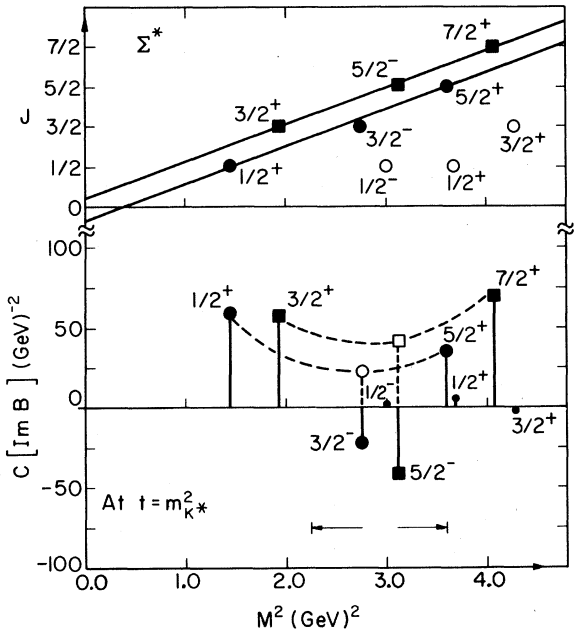

FIG. 13. Exchange degeneracy of low-energy Σ^* resonances. The upper half shows Σ_α, Σ_β, Σ_δ, Σ_γ baryon states on two, rather than four, trajectories. Lower spin states are indicated with open circles. The lower half of the figure shows contributions to the ImB sum rule at $t = m_K{}^{*2}$. The contributions along each trajectory are seen to vary smoothly, apart from the EXD alternation in sign. The interval indicated by arrows is the range covered in the analysis of Ferro-Luzzi *et al.* (Ref. 33).

for the reaction $K^- n \to \pi^- \Lambda$ and its line-reversed reaction $\pi^+ n \to K^+ \Lambda$. To the contrary, however, experiments indicate that at energies near $p_{\text{lab}} \approx 4.0$ GeV/c the slope of $d\bar{\sigma}/dt$ is approximately twice as steep as the slope of $d\sigma/dt$ and the integrated cross section $\bar{\sigma}$ is considerably smaller than σ. The data on the slope parameter for both reactions are shown in Fig. 9. Even more embarrassing is the evidence[35,36] shown in Fig. 14 that the polarizations for the two reactions have the *same* sign, at least for $|t| < 0.4$ (GeV/c)^2. Such behavior of the polarization is impossible for a model with only one effective pole of each signature because then it is always true that $\bar{P} d\bar{\sigma}/dt \approx -P d\sigma/dt$. This is independent of whether or not there is weak EXD of the trajectories. The assumption of one effective pole of each signature is evidently too simple at intermediate energies.[37] The energy dependence of the slope parameters in Fig. 9 indicates that at higher momenta [$p_{\text{lab}} > 6.5$ GeV/c, $s > 13$ (GeV)^2] two weakly EXD effective Regge poles may be an adequate description, since the slopes for $\pi^+ n \to K^+ \Lambda$ and $K^- n \to \pi^- \Lambda$ tend to become equal. It remains to be seen whether the polarizations for the two reactions have opposite signs at these higher momenta, and whether the magnitudes of the integrated cross sections approach each other.

Why does our FESR calculation with two effective Regge poles fit the $K^- n \to \pi^- \Lambda$ data at intermediate energies, but fail to fit the data on $\pi^+ n \to K^+ \Lambda$? The reader may well say that the data obviously do not permit a description with only two Regge poles and that, since we chose to fit $K^- n \to \pi^- \Lambda$, we necessar-

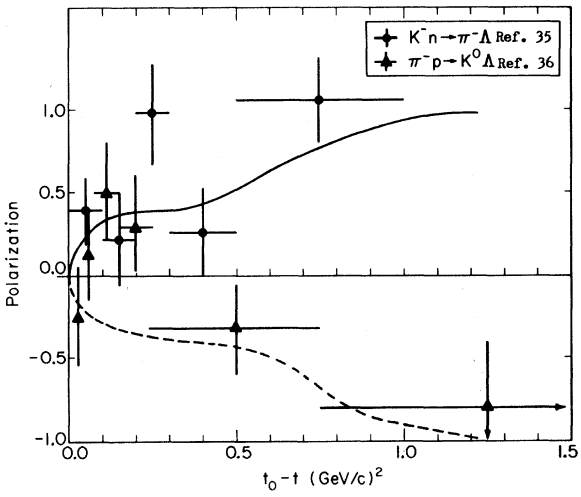

FIG. 14. Comparison of polarization at 3.9 GeV/c. Solid and dashed curves are the results of our calculation for $K^- n \to \pi^- \Lambda$ and $\pi^+ n \to K^+ \Lambda$, respectively. At small $|t|$, the observed polarizations have the same sign, contrary to our predictions or those of any model involving only one Regge pole of each signature.

ily fail for $\pi^+n\to K^+\Lambda$. There is clearly some truth in such a statement, but it is misleading. We tried the alternative of fitting the differential cross section for $\pi^+n\to K^+\Lambda$ at 3–4 GeV/c. Even with wide variation of the $\frac{1}{2}^+$ octet couplings and also coupling of the $\Sigma(1385)$, it proved impossible to make the forward peak of $d\bar{\sigma}/dt$ sharp enough to agree with experiment. We are thus still with the question, why does our sum-rule calculation, oversimplified though it may be, work at 3–6 GeV/c for $K^-n\to\pi^-\Lambda$ and not for $\pi^+n\to K^+\Lambda$? The character of the s-channel and u-channel resonances in the sum rules sheds some light on this question. From Table I and Fig. 13 it can be inferred that the dominant s-channel resonances ($K^-n\to\pi^-\Lambda$) are "peripheral" resonances whose angular momenta increase with their masses, and whose s-channel nonflip and spin-flip helicity amplitudes have zeros at roughly the same t values as $J_0(R(-t)^{1/2})$ and $J_1(R(-t)^{1/2})$, respectively, where $R\approx 0.9$ fm.[38] This behavior is analogous to an elastic reaction, and is not surprising in view of the exothermic nature of the process. On the other hand, the threshold for $\pi^+n\to K^+\Lambda$ is 530 MeV above the threshold, $m_N+m_\pi=1079$ MeV, for elastic π^+n scattering. Centrifugal barrier effects will hinder peripheral πN resonances from contributing to the inelastic reaction $\pi^+n\to K^+\Lambda$. The dominant u-channel contributions are thus expected to come from πN states of relatively small spin, "nonperipheral" resonances. This is indeed what is seen from Tables I and IV. The "peripheral" resonances, $D15$ and $F15$, which are very important in the sum rules for elastic πN scattering, couple weakly to $\pi^+n\to K^+\Lambda$, while the "nonperipheral" states such as $N(1700)$ $\frac{1}{2}^-$ and $N(1860)$ $\frac{3}{2}^+$ [and the $N(938)$ $\frac{1}{2}^+$ pole] are of considerable importance.

Let us assume that a high-energy model with two effective Regge poles which are approximately weakly EXD is a reasonable description of both reactions at incident momenta above 6–8 GeV/c, but fails for momenta of order 3–4 GeV/c. We are then led to the following hypothesis:

(1) The leading t-channel Regge singularities (called effective poles above) are dual to the "peripheral" resonances in the direct channel.

(2) Lower-lying t-channel j-plane singularities are dual to the "nonperipheral" resonances in the direct channel.

As can be seen from the energy denominators in a fixed-t dispersion relation, at intermediate energies the contributions to the real part of a reaction amplitude from the resonances in that channel are more important than those from resonances in the crossed channel. Since the "peripheral" resonances occur in the $K^-n\to\pi^-\Lambda$ channel, we can understand why the simple two-pole model works even at intermediate energies for that channel.[39] The dominance of "nonperipheral" states for $\pi^+n\to K^+\Lambda$ on the other hand argues for a more complicated description at intermediate energies.

There is an apparent inconsistency here that should be dispelled. At intermediate energies $\pi^+n\to K^+\Lambda$ is *more peripheral* than $K^-n\to\pi^-\Lambda$. This seems to contradict the dominance of "nonperipheral" states in the resonance region of $\pi^+n\to K^+\Lambda$ and of "peripheral" states in $K^-n\to\pi^-\Lambda$. Such arguments work for *elastic* processes, but not for inelastic reactions where the resonant contributions enter with different signs in general. For inelastic reactions it appears that no simple correlation can be established between the peripherality of the resonance contributions and the sharpness of the diffraction peak.

(Note added in proof. A hybrid calculation using imaginary parts of amplitudes from the FESR and real parts calculated from the fixed-t dispersion relations confirms the arguments of the two preceding paragraphs and gives a semiquantitative description of the different slopes of the two cross sections at 2–5 GeV/c.)

The association of "nonperipheral" resonances with lower-lying j-plane singularities in a crossed channel can be made plausible by considering the idealized explicitly dual Veneziano amplitude. Our distinction between "peripheral" and "nonperipheral" contributions is in some ways analogous to Harari's description of elastic scattering.[38] It differs, however, in that his "nonperipheral" contributions, arising mainly from the direct-channel background, build up the Pomeranchon singularity. At high energies, the Pomeranchon part is what survives for elastic processes. In our inelastic reactions we assume that the nonperipheral part is less and less important as the energy increases. There is no inconsistency between our view and Harari's. The idea that "nonperipheral" resonances are dual to lower-lying Regge singularities can be incorported into Harari's scheme with no difficulty.

The reader will have noted that we did not attribute the breakdown of EXD and other peculiarities of the two reactions to high-lying cuts in the j plane. Some reasons are:

(1) The hint from Fig. 9 of the improvement of EXD at higher energies argues against important Regge-cut contributions that distinguish between the two reactions.

(2) Pomeranchon-Regge pole cuts calculated in EXD models give effects opposite to what is seen experimentally. On the other hand, lower-lying Reggeon-Reggeon cuts may contribute with the correct sign.[40]

(3) The sum rules can be viewed as giving the behavior of the leading effective Regge singularities

whatever they are.

(4) Within a sum-rule calculation of the sort necessary here, nothing can be inferred about the specific nature of the j-plane singularities.

IV. SUMMARY

Using FESR for the reactions $K^-n \to \pi^-\Lambda$ and $\pi^+n \to K^+\Lambda$, we determine the effective "pole" parameters of the K^* and K^{**} Regge trajectories from a knowledge of the low-energy resonances and their couplings. The resonance parameters and the $D/(D+F)$ ratio for the $\frac{1}{2}^+$ baryon octet are varied somewhat to test the sensitivity of the high-energy predictions; $\frac{1}{2}^+$ octet couplings within the range of values found empirically in other reactions are preferred in our solution. We find that the s-channel resonances in $K^-n \to \pi^-\Lambda$ *do* add in such a way as to produce predominately real amplitudes at high energies as predicted by duality diagrams. We find, however, that these predictions are not satisfied *exactly*. Although the phases of both A' and B are small and independent of t for $|t| < 0.5$ $(\mathrm{GeV}/c)^2$, the residues of the even- and odd-signature Regge poles are closely exchange degenerate only for the B amplitudes, and not for the A' amplitudes, thereby allowing an appreciable polarization for $K^-n \to \pi^-\Lambda$ as is observed experimentally.

The Regge-pole parameters determined from the sum rules give a good fit to the reaction $K^-n \to \pi^-\Lambda$ over a wide range of energies, whereas they are unable to fit $\pi^+n \to K^+\Lambda$ at intermediate energies. Comparison of the resonance contributions to $K^-n \to \pi^-\Lambda$ and $\pi^+n \to K^+\Lambda$ shows that "peripheral" resonances dominate the sum rules in the first reaction, while "nonperipheral" states are important in the second. By supposing that "peripheral" resonances are dual to the leading Regge singularities in the t channel, while "nonperipheral" resonances are dual to lower-lying singularities, we are led to a rationale of why the simple model of two effective Regge poles is adequate for $K^-n \to \pi^-\Lambda$ even at intermediate energies, but inadequate there for $\pi^+n \to K^+\Lambda$.

---

†Work supported in part by the U. S. Atomic Energy Commission.

[1]H. Harari, Phys. Rev. Letters 22, 562 (1969).

[2]J. L. Rosner, Phys. Rev. Letters 22, 689 (1969).

[3]R. Barloutaud, Duong Nhu Hoa, J. Griselin, D. W. Merrill, J. C. Scheuer, W. Hoogland, J. C. Kluyver, A. Minguzzi-Ranzi, A. M. Rossi, B. Haber, E. Hirsch, J. Goldberg, and M. Laloum, Nucl. Phys. B9, 493 (1969).

[4]W. L. Yen, A. C. Ammann, D. D. Carmony, R. L. Eisner, A. F. Garfinkel, L. J. Gutay, S. L. Kramer, and D. H. Miller, Phys. Rev. Letters 22, 963 (1969).

[5]Kwan-Wu Lai and James Louie, Nucl. Phys. B19, 205 (1970).

[6]See, for example, J. D. Jackson, Rev. Mod Phys. 42, 12 (1970).

[7]V. Singh, Phys. Rev. 129, 1889 (1963).

[8]D. Z. Freedman and J. Wang, Phys. Rev. 153, 1596 (1967).

[9]A. Barbaro-Galtieri, in *Hyperon Resonances-70,* edited by E. C. Fowler (Moore, Durham, N. C., 1970), p. 173.

[10]P. J. Litchfield, in *Hyperon Resonances-70,* edited by E. C. Fowler (Moore, Durham, N. C., 1970), p. 215.

[11]CERN-Heidelberg collaboration, presented by D. E. Plane in, *Hyperon Resonances-70,* edited by E. C. Fowler (Moore, Durham, N. C., 1970), p. 123.

[12]A. Berthon, L. K. Rangan, J. Vrana, I. Butterworth, P. J. Litchfield, A. M. Segar, J. R. Smith, J. Meyer, E. Pauli, and B. Tallini, Nucl. Phys. B20, 476 (1970).

[13]G. F. Cox, G. S. Islam, D. C. Colley, D. Eastwood, J. R. Fry, F. R. Heathcote, D. J. Candlin, J. G. Colvine, G. Copley, N. E. Fancey, J. Muir, W. Angus, J. R. Campbell, W. T. Morton, P. J. Negus, S. S. Ali, I. Butterworth, F. Fuchs, D. P. Goyal, D. B. Miller, D. Pearce, and B. Schwarzschild, Nucl. Phys. B19, 61 (1970).

[14]W. S. Smart, Phys. Rev. 169, 1330 (1968); W. S. Smart, A. Kernan, G. E. Kalmus, and R. P. Ely, Phys. Rev. Letters 17, 556 (1966).

[15]J. Edwin Rush, Jr., Phys. Rev. 173, 1776 (1968); S. R. Deans, W. G. Holladay, and J. E. Rush, paper submitted to the Fourteenth International Conference on High-Energy Physics, Vienna, 1968 (unpublished).

[16]S. Orito and S. Sasaki, Lett. Nuovo Cimento 1, 936 (1969); S. Orito, Tokyo report, 1969 (unpublished).

[17]F. Wagner and C. Lovelace, Nucl. Phys. B25, 411 (1971).

[18]Particle Data Group, Rev. Mod. Phys. 42, 87 (1970).

[19]R. L. Warnock and G. Frye, Phys. Rev. 138, B947 (1965).

[20]N. Zovko, Phys. Letters 23, 143 (1966).

[21]J. K. Kim, Phys. Rev. Letters 19, 1079 (1967). Note, however, that we have corrected Kim's results as explained by C. H. Chan and F. T. Meiere, Phys. Rev. Letters 20, 568 (1968).

[22]R. Levi-Setti, in *Proceedings of the Lund International Conference on Elementary Particles,* edited by G. von Dardel (Berlingska, Lund, Sweden, 1970), p. 341.

[23]C. H. Chan and F. T. Meiere, Phys. Letters 28B, 125 (1968).

[24]For the $\Sigma(1197)$ pole the product of coupling constants found in this way happens to be closely the same as the product of Kim's value for $g(\Sigma^- \to K^- p)$ and Chan and Meiere's value for $g(\Sigma^0 \to \pi^0\Lambda)$.

[25]The sum $\mathbf{S}\,(A'^{(+)}, 0)$ vanishes at two places on the interval $0 < |t| < 1$ $(\mathrm{GeV}/c)^2$, one near $|t| = 0.1$ and another near $|t| \simeq 0.6$. Identifying $\alpha^+ = 0$ at $|t| \simeq 0.6$ not only is contrary to expectations based on a linear trajectory of reasonable slope and the observed K^{**} mass, but also gives an unacceptable dip in $d\sigma/dt$ at $t = 0$.

[26]We emphasize here that, although the residues themselves depend on the choice of ν_0, the high-energy ob-

servables are completely independent of this choice. The observables do depend on ν_1, however.

[27]L. Wolfenstein, Phys. Rev. 96, 1654 (1954). See also E. L. Berger and G. C. Fox, Phys. Rev. Letters 25, 1783 (1970).

[28]A. D. Brody, W. B. Johnson, D. W. G. S. Leith, J. S. Loos, G. J. Luste, K. Moriyasu, B. C. Shen, W. M. Smart, F. C. Winkelmann, R. J. Yamartino, and B. Kehoe, SLAC Report No. SLAC-PUB-823, 1970 (unpublished).

[29]The more nearly EXD behavior at high energies of the B amplitude than the A' is popularly understood in terms of Regge-cut contributions [see G. C. Fox, in *High Energy Collisions*, Third International Conference held at State University of New York, Stony Brook, 1969, edited by C. N. Yang, J. A. Cole, M. Good, R. Hwa, and J. Lee-Franzini (Gordon and Breach, New York, 1969), p. 367.

[30]The actual size of the polarization depends not only on the phase difference, but also on the magnitude of the product $|A'B|$. From Fig. 10 it can be seen that Eq. (2.12) is approximately satisfied at $t \simeq 0$.

[31]R. Dolen, D. Horn, and C. Schmid, Phys. Rev. 166, 1768 (1968).

[32]See also C. Schmid and J. K. Storrow, Nucl. Phys. B29, 219 (1971). These authors give arguments to justify the testing of EXD for the s-channel states at $t \geq m_{K^*}{}^2$. The qualitative features displayed in Fig. 13 also hold at $t \approx 0$ for ImB, and equally for ImA'.

[33]M. Ferro-Luzzi, H. K. Shepard, A. Kernan, R. T. Poe, and B. C. Shen, University of California, Riverside, Report No. UCR-P107-114, 1970 (unpublished).

[34]See the Appendix of Ref. 6 for the meaning of these and other technical terms.

[35]D. J. Crennell, Uri Karshon, Kwan Wu Lai, J. S. O'Neall, J. M. Scarr, R. M. Lea, T. G. Schumann, and E. M. Urvater, Phys. Rev. Letters 23, 1347 (1969).

[36]M. Abramovich, H. Blumenfeld, V. Chaloupka, S. U. Chung, J. Diaz, L. Montanet, J. Pernegr, S. Reucroft, J. Rubio, and B. Sadoulet, Nucl. Phys. B27, 477 (1971).

[37]The discrepancies at intermediate energies are currently "explained" by invoking Regge cuts in addition to poles. A. Krzywicki and J. Tran Thanh Van, Phys. Letters 30B, 185 (1969) are able to fit the behavior of the polarization shown in Fig. 14 by such means.

[38]H. Harari, Ann. Phys. (N.Y.) 63, 432 (1971), and SLAC Report No. SLAC-PUB-837, 1970 (unpublished).

[39]The shrinkage of the forward peak shown by the SLAC data (Ref. 28) (see Fig. 9) lends circumstantial support to a description of $K^-n \to \pi^-\Lambda$ by Regge poles with little further complication.

[40]For some model calculations, see Chris Quigg, Ph. D. thesis, LRL Report No. UCRL-20032, 1970 (unpublished).

PHYSICAL REVIEW D VOLUME 4, NUMBER 3 1 AUGUST 1971

Rotation of the Symmetry Axis in K-π Scattering*

W. E. Slater
Department of Physics, University of California at Los Angeles, Los Angeles, California 90024
(Received 12 April 1971)

The failure of the Treiman-Yang test of one-pion exchange in the reactions $K^+p \to K^0\pi^0\Delta^{++}$ and $K^+\pi^-\Delta^{++}$ for c.m. energies from 2.5 to 5.0 GeV is shown to have a simple dependence on t'. We find an empirical dynamic z axis with respect to which the K-meson angular distributions are independent of azimuth. This axis, which depends on t', is seen to be equivalent to the axis of Donohue and Högaasen in the neighborhood of the $K^*(0.89)$.

In a calculation based on the absorption model of Gottfried and Jackson,[1] Donohue and Högaasen[2] suggested the use of a "dynamic" reference frame in which the density matrix describing the decay of a vector meson (e.g., ρ or K^*) is diagonal. This frame differs from the usual t-channel (Jackson) frame[3] by a rotation. Experimentally, such effects have been noted in several final states[4] of reactions induced by π^+ mesons and photons on hydrogen. We first noted the rotation in a sample of 4850 events of reaction (1a) and 703 events of reaction (1b) at 7.3 GeV/c,

$$K^+p \to K^+\pi^-\Delta^{++}, \tag{1a}$$

$$K^+p \to K^0\pi^0\Delta^{++}. \tag{1b}$$

To confirm the existence of the effect and to look at the s, t, and $M_{K\pi}$ dependences, we have used the world K^+p collaboration data[5] consisting of 37 152 events of reaction (1a) and 6592 events of reaction (1b). We note that analogous effects, *prima facie*, have been understood in the angular distribution of photons produced by inelastic scattering of protons on nuclei[6]; a simple model leading to the same effect in inelastic α-nucleus scattering was described by Inglis[7] and this rotation was observed in many experiments.[8]

If one assumes that a single-pion-exchange mechanism dominates the low-momentum-transfer $[t=(P_{\text{target}}-P_\Delta)^2]$ region of reactions (1), as in Fig. 1(a), then an appropriate coordinate system in which to study the final-state K-meson angular distribution was defined by Jackson[3] such that the